The physics models of FLUKA: status and recent developments

CHEP03
La Jolla, March 2003

F. Ballarini[1], G. Battistoni[2], F. Cerutti[2], A. Empl[3], A. Fassò[4], A. Ferrari[5], E. Gadioli[2], M.V. Garzelli[2], A. Ottolenghi[1], J. Ranft[6], S. Roesler[7], P.R. Sala[8]

[1] INFN and Pavia University, [2] INFN and Milan University, [3] Houston University, [4] GSI and CERN, [5] INFN and CERN, [6] Siegen University, [7] CERN, [8] INFN and ETH Zurich

FLUKA

Interaction and transport Monte Carlo code

- Hadron-hadron and hadron-nucleus interactions 0-10000 TeV
- Nucleus-nucleus interactions 0-10000 TeV/n
- Electromagnetic and μ interactions 1 keV-10000 TeV
- Neutrino interactions
- Charged particle transport including all relevant processes
- Transport in magnetic field
- Combinatorial (boolean) and Voxel geometry
- Neutron multigroup transport and interactions 0-20 MeV
- Analog calculations, or with variance reduction

Design philosophy: the highest priorities

⋆ Sound and modern physics

- Based, as far as possible, on original and well tested microscopic models
- All steps (Glauber-Gribov cascade, (G)INC, preequilibrium, evaporation/fragmentation/fission) are self-consistent and have solid physical bases
- Performances optimized by comparing with experimental data at single interaction level: "theory driven, benchmarked with data"
- No tuning whatsoever on "integral" data, such as calorimeter resolutions, thick target yields etc.
- Final predictions obtained with minimal free parameters fixed for all energies/target/projectiles
- Results in complex cases, as well as properties and scaling laws, arise naturally from the underlying physical models
- Basic conservation laws fulfilled "a priori"
- Correlations preserved fully within interactions and among shower components

$\Longrightarrow$ Predictivity where no experimental data are directly available

Design philosophy: the highest priorities

⋆ Self-consistency

- Full cross-talk between all components:
  hadronic, electromagnetic, neutronic, muonic
- Effort to achieve the same level of accuracy
  for each component
  for all energies (from thermal to thousands of TeV)

⋆ Numerical accuracy

- Optimized computer algorithms to implement the FLUKA physical models and the geometry tracking
- Choice of the best available atomic and nuclear data
- Systematic use of relativistic kinematics

Result: Energy conserved within 10^{-10} !

EMF: ElectroMagnetic Fluka

- Photoelectric: shell by shell cross sections, fluorescence, angular distribution, Auger, polarization
- Compton and Rayleigh: atomic bonds, polarization
- Pair production: correlated angular and energy distribution; also for μ
- Photonuclear: all energies and all isotopes: GDR, QD, VMD; also for μ
- Bremsstrahlung: full set of cross sections from Berger and Seltzer for 100 elements interpolated to a finer energy mesh, LPM, Ter-Mikaelyan, correlated angular and energy distribution, finite at tip, also for μ
- Bhabha and Møller scattering
- Positron annihilation: at rest and in flight, photon polarization
- μ^- capture at rest
- Optical photons (Cerenkov, scintillators): production and transport

Charged particle transport

- δ-ray production. Below δ threshold: Ionization energy losses with fluctuations
- Ionization fluctuations: new general approach based on the cumulants of a distribution
- Ionization potential and density effect parameters: latest recommended values, can be overridden by user
- Heavy ions:
  - Effective charge with fluctuations
  - Charge exchange effets (dominant at low energies, ad-hoc FLUKA model)
- Positron dE/dx: radiation integral scaled according to Kim et al., differential cross sections fitted to numerical results of Feng et al.
- Multiple Coulomb scattering: path length correction, lateral displacement, angle correlation, soft approach to boundaries, screening and spin-relativistic corrections, fully coupled to magnetic field transport
- Single scattering at boundaries and when Molière theory conditions are not satisfied. Also systematic if requested

The FLUKA hadronic models

Hadron-Nucleon

Elastic, exchange	P<3-5GeV/c	low E π,K	High Energy
Phase shifts, data, eikonal	Resonance prod. and decay	Special	DPM hadronization

Hadron-Nucleus

P<4-5GeV/c	High Energy
PEANUT: Sophisticated GINC preequilibrium	Glauber-Gribov multiple interactions Coarser GINC

Evaporation/Fission/Fermi break-up

γ deexcitation

Inelastic hN at high energies: (DPM, QGSM, ...)

- Problem: "soft" interactions $\rightarrow$ no perturbation theory
- Solution: Interacting strings (quarks held together by the gluon-gluon interaction into the form of a string)
- Interactions treated in the Reggeon-Pomeron framework
- At sufficiently high energies the leading term corresponds to a Pomeron ($I\!P$) exchange (a closed string exchange)

- Each of the two colliding hadrons splits into two colored partons $\rightarrow$ combination into two color neutral chains $\rightarrow$ two back-to-back jets
- Physical particle exchange produce single chains at low energies
- Higher order contributions with multi-Pomeron exchanges important at $E_{lab} \geq 1$ TeV

Glauber

⋆ Glauber cascade

- Quantum mechanical method to compute all relevant cross sections from hadron–nucleon scattering and nuclear ground state wave function
- Elastic, Quasi-elastic and Absorption hA cross sections derived from Free hadron-Nucleon cross section + Nuclear ground state ONLY

⋆ Glauber-Gribov

- Field theory formulation of Glauber model
- Multiple collision terms ⇔ Feynman graphs
- High energies: exchange of one or more Pomerons ($I\!P$) with one or more target nucleons (a closed string exchange)

⋆ Special effects

- Formation zone (= materialization time)
- Coherence length for elastic or quasielastic interactions (similar to LPM)
- π-nucleus medium effects: the produced Δ can undergo:
  decay ⇒ elastic scattering/charge exchange
  absorption ⇒ π is absorbed ⇒ the width of the free resonance is modified

DPM

★ DPM provides recipes for:

- determining the number of cut $I\!P$omerons, and therefore the number of chains contributing to the reaction
- forming the chains using the valence and possibly sea quarks of the two colliding hadrons
- determining the energy and momentum carried by each chain, according to the momentum distribution functions of the two colliding hadrons
- hadronizing each chain producing the final hadrons, stable ones or resonances

★ Hadronization: not exactly a part of DPM, but DPM is factorized so that it can admit any suitable hadronization scheme (hard processes, $e^+e^-\ldots$)

- Hadronization properties assumed to be independent of the physical process originating the chain (chain universality)
- Excluding hadronization, little or no freedom in each individual step
  $\Rightarrow$ high predictive power of the model
- Diffractive scattering in h–h, h–N and N–N collisions can also be described in the DPM framework

From resonance production to DPM

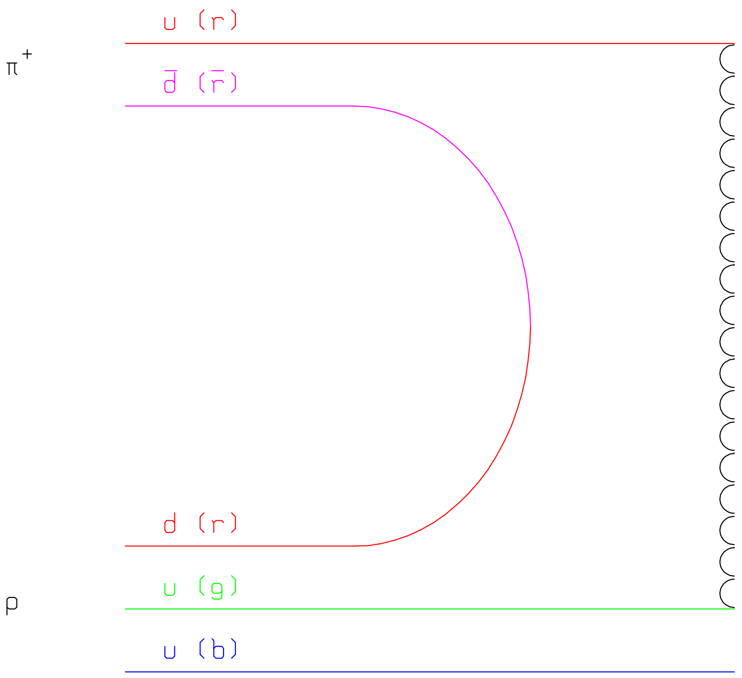

Single chain diagram for $\pi^+ - p$ scattering, corresponding to a physical particle exchange. The color (red, blue, and green) and quark combination shown in the figure is just one of the allowed possibilities

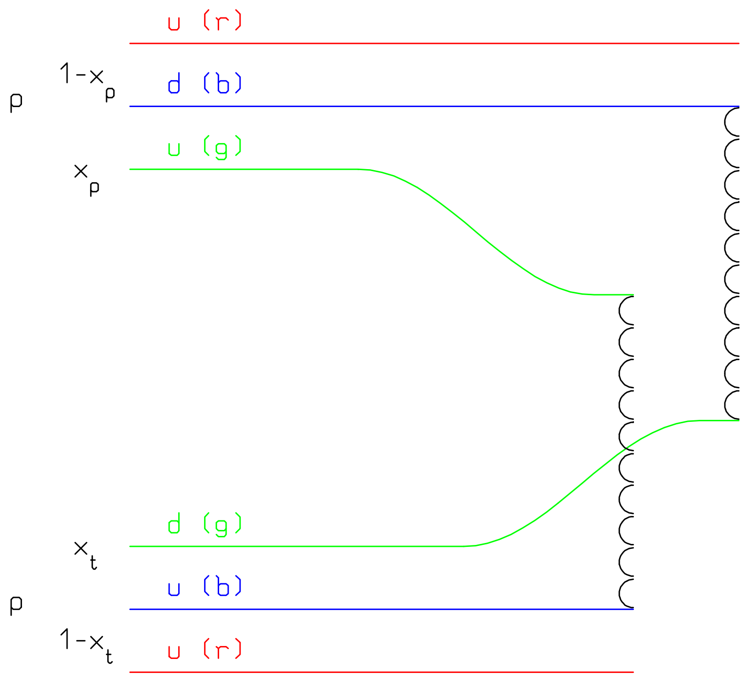

Leading two-chain diagram in DPM for $p - p$ scattering. The color (red, blue, and green) and quark combination shown in the figure is just one of the allowed possibilities

DPM: chain examples

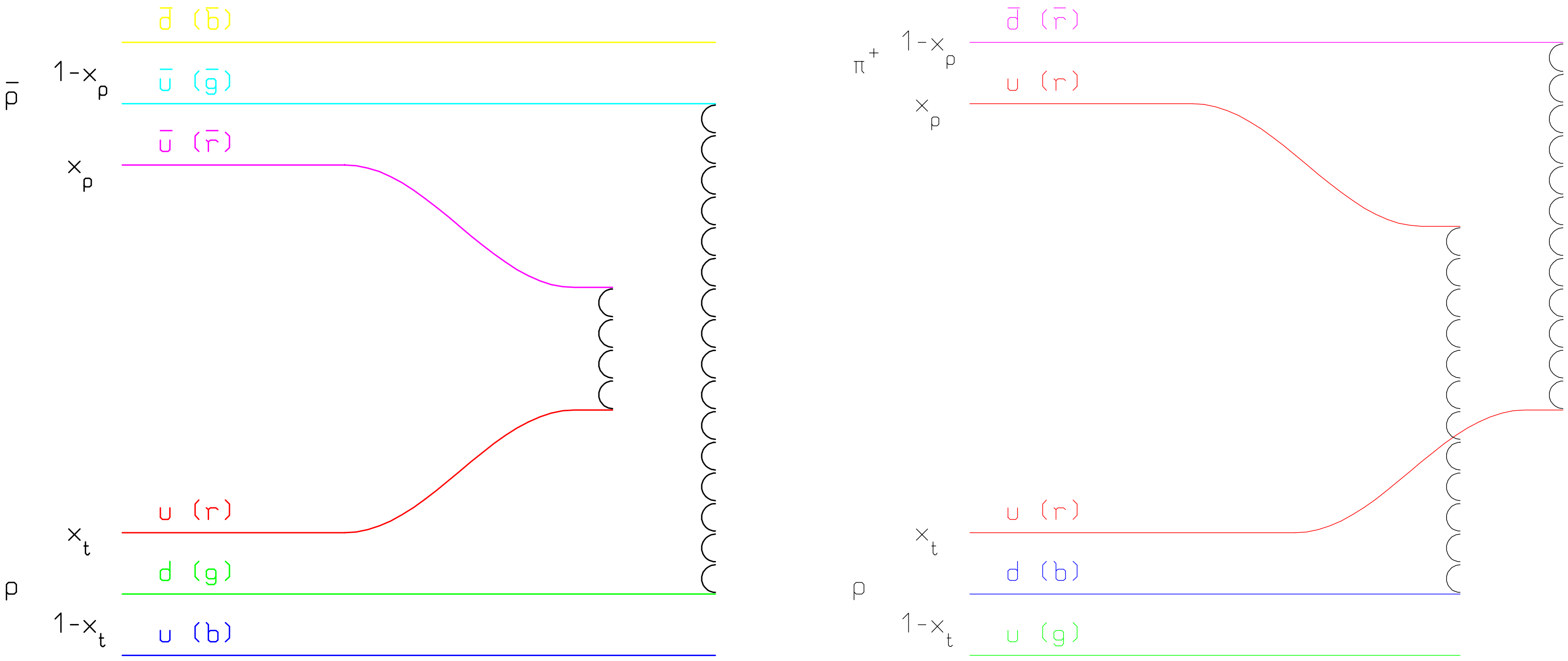

Leading two-chain diagrams in DPM for $p - \bar{p}$ (left) and $\pi - p$ (right) scattering. The color (red, blue, and green) and quark combinations shown in the figure are just one of the allowed possibilities

Nonelastic hN high E: (π^+ p) 250 GeV, x_F and p_t

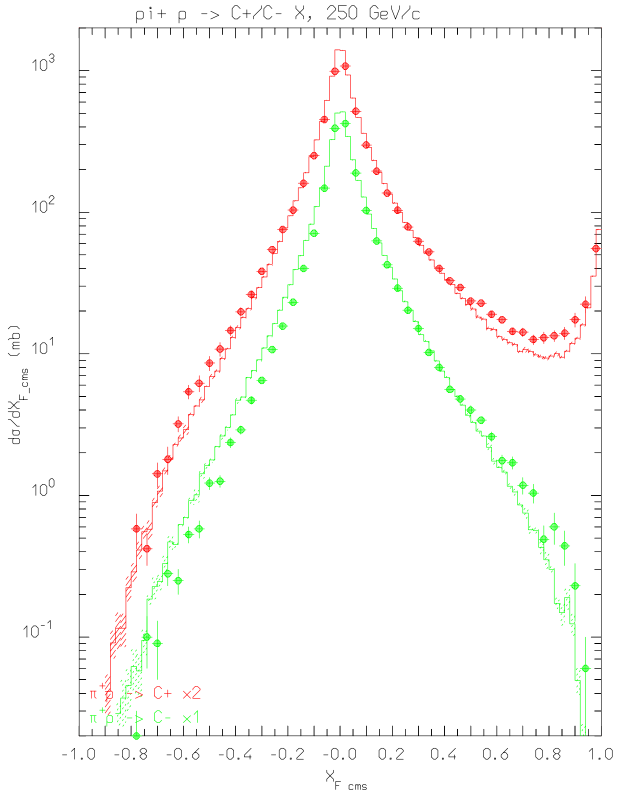

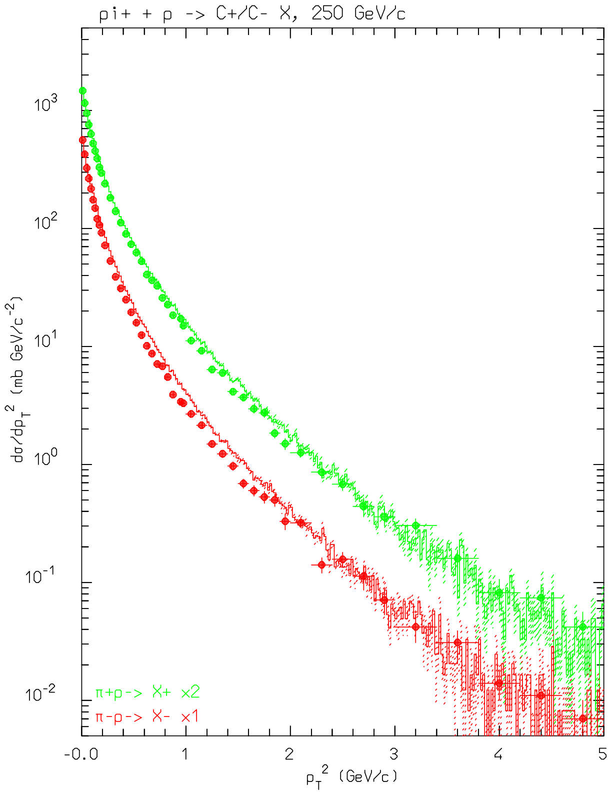

Distributions of positive particles and π^- produced by 250 GeV/c π^+ incident on a hydrogen target.

Left:: Feynman x_F^* spectrum; Right: p_t spectrum

Experimental data (symbols) from M. Adamus et al. ZPC39, 311 (1988)

h-A at high energies: Glauber-Gribov

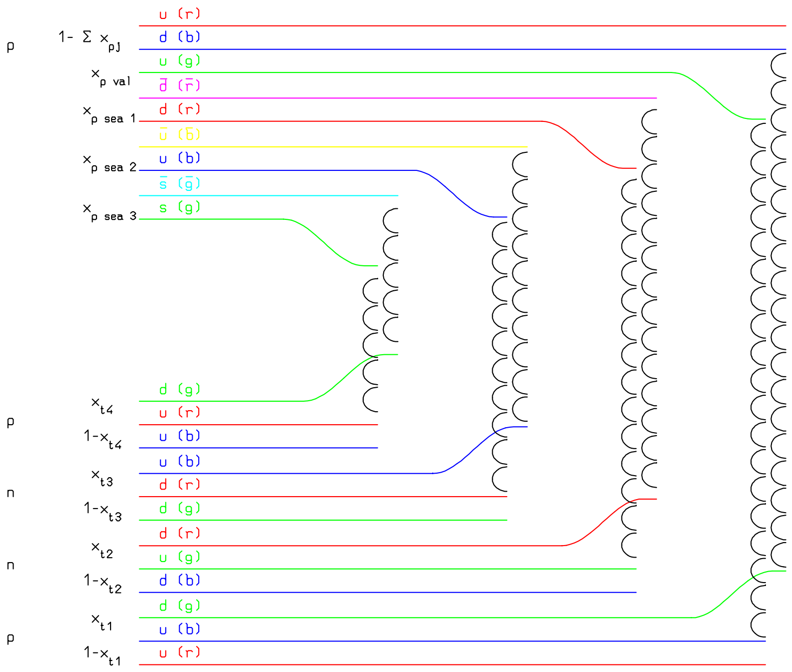

One of the possibilities for Glauber-Gribov scattering with 4 collisions

Gribov

$\Downarrow$

2ν chains

2 valence-valence chains

$2(\nu - 1)$ chains between projectile sea and target valence (di)quarks.

No freedom, except in mass effects at low energies.

Fermi motion included $\rightarrow$ smearing of E and p_T distributions

Nonelastic hA interactions at high energies: examples

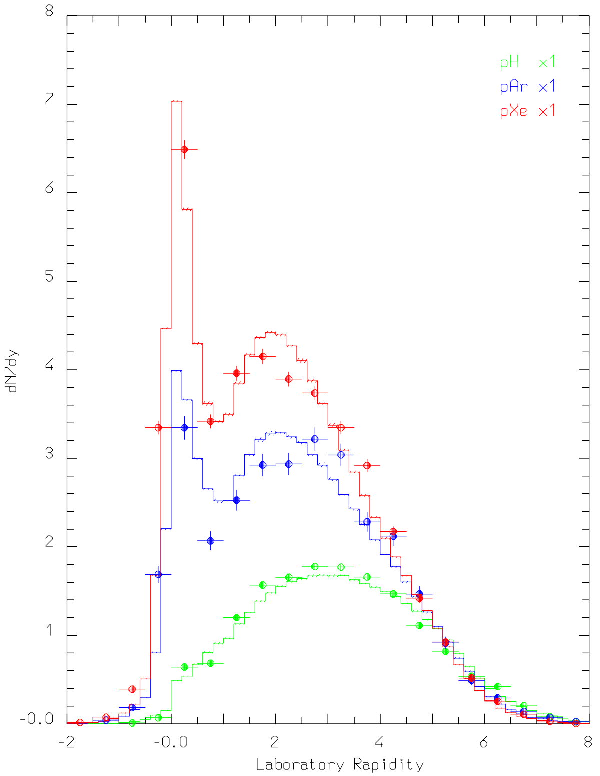

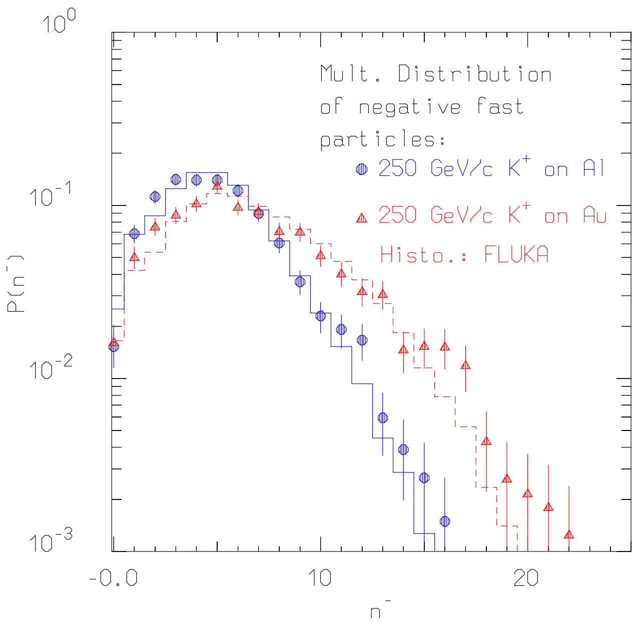

Left: Rapidity distribution of charged particles produced in 200 GeV proton collisions on H, Ar and Xe

Data from C. De Marzo et al., PRD26, 1019 (1982)

Right: Multiplicity distribution of negative shower particles for 250 GeV/c K^+ on Al and Au

Data from I.V. Ajinenko et al. ZPC42 377 (1989) and N.M. Agababyan et al. ZPC50 361 (1991)

Nonelastic hA interactions at high energies: examples

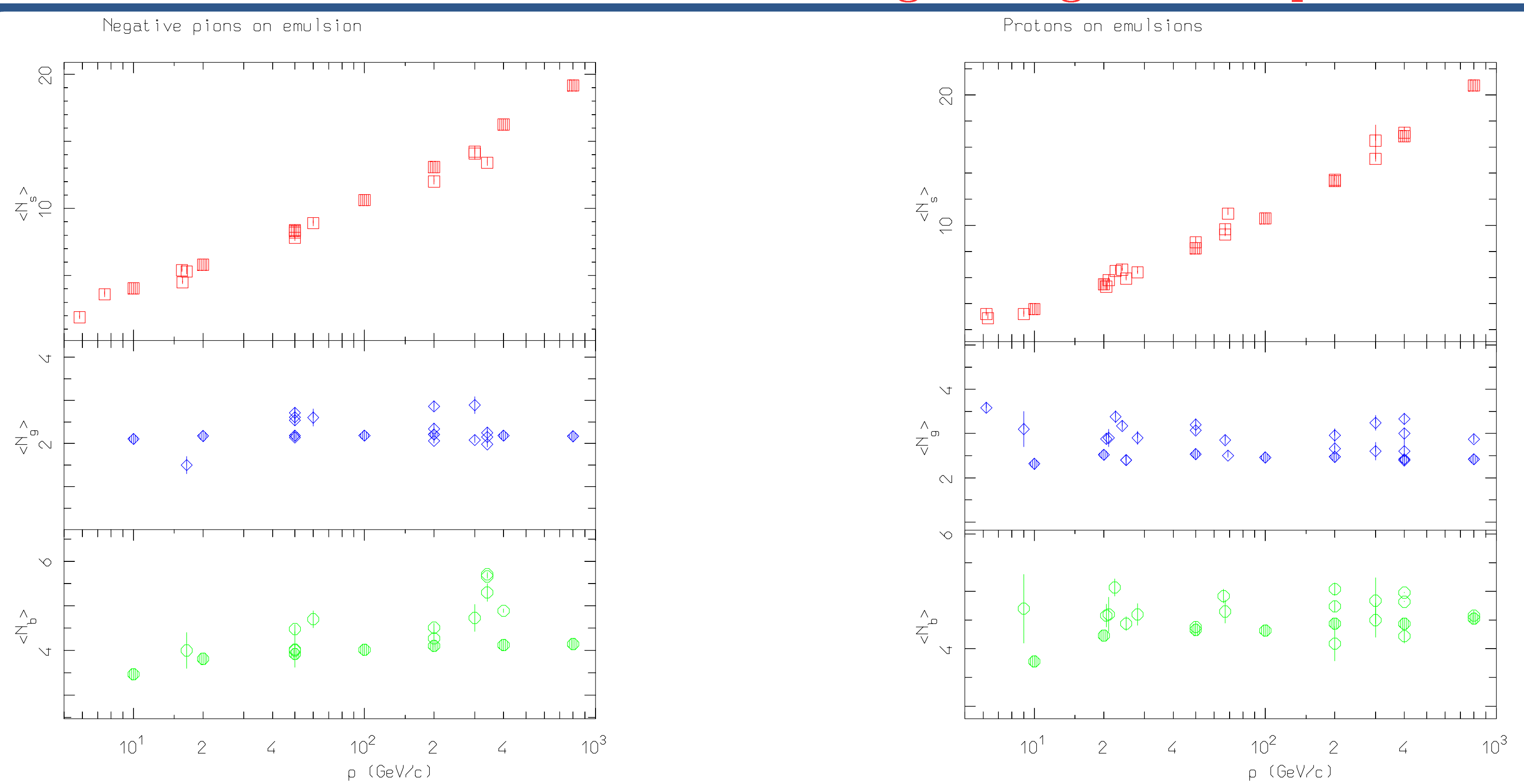

Shower, grey, and black tracks multiplicities for π^- (left) and protons (right) incident on emulsion
Open symbols: experimental data from various sources, full symbols: FLUKA results

The ≈ logarithmic increase of "fast" tracks (from projectile primary interactions), and the saturation of "grey" (INC reinteractions) and "black" (evaporation) tracks are well predicted by the Glauber cascade model + Formation zone.

Generalized Intra-Nuclear Cascade **IS NOT** Bertini

⋆ Although a distant descendant of the crude (but still popular!) “Bertini model” of the ’70s (implemented in the Oak Ridge HETC code), GINC does not share its many weaknesses:

- Bad behavior for projectile energies $\leq$ 100–200 MeV
- Constant binding energy
- Bad behavior at backward angles
- Coulomb barrier effects neglected
- No potential effects (= no refraction and reflection)
- No formation zone
- No Glauber cascade
- Transport of secondaries below all safe limits imposed by theory

Generalized Intra-Nuclear Cascade

⋆ Main assets of the full GINC as implemented in FLUKA below 4 GeV:

- PEANUT (PreEquilibrium Approach to NUclear Thermalization): preequilibrium stage handling nucleons, pions, kaons, γ, stopping μ^-
- Nucleus divided into 16 radial zones of different density, plus 6 outside the nucleus to account for nuclear potential, plus 10 for charged particles
- Different nuclear densities for neutrons and protons
- Nuclear (complex) optical potential $\Longrightarrow$ curved trajectories in the mean nuclear+Coulomb field (reflection, refraction)
- Updating binding energy (from mass tables) after each particle emission
- Relativistic kinematics
- Energy-momentum conservation including the recoil of the residual nucleus
- Nucleon Fermi motion
- Quantum effects (mostly suppressing): Pauli blocking, Formation zone, Nucleon antisymmetrization, Nucleon-nucleon hard-core correlations, Coherence length

Microscopic pion absorption cross sections

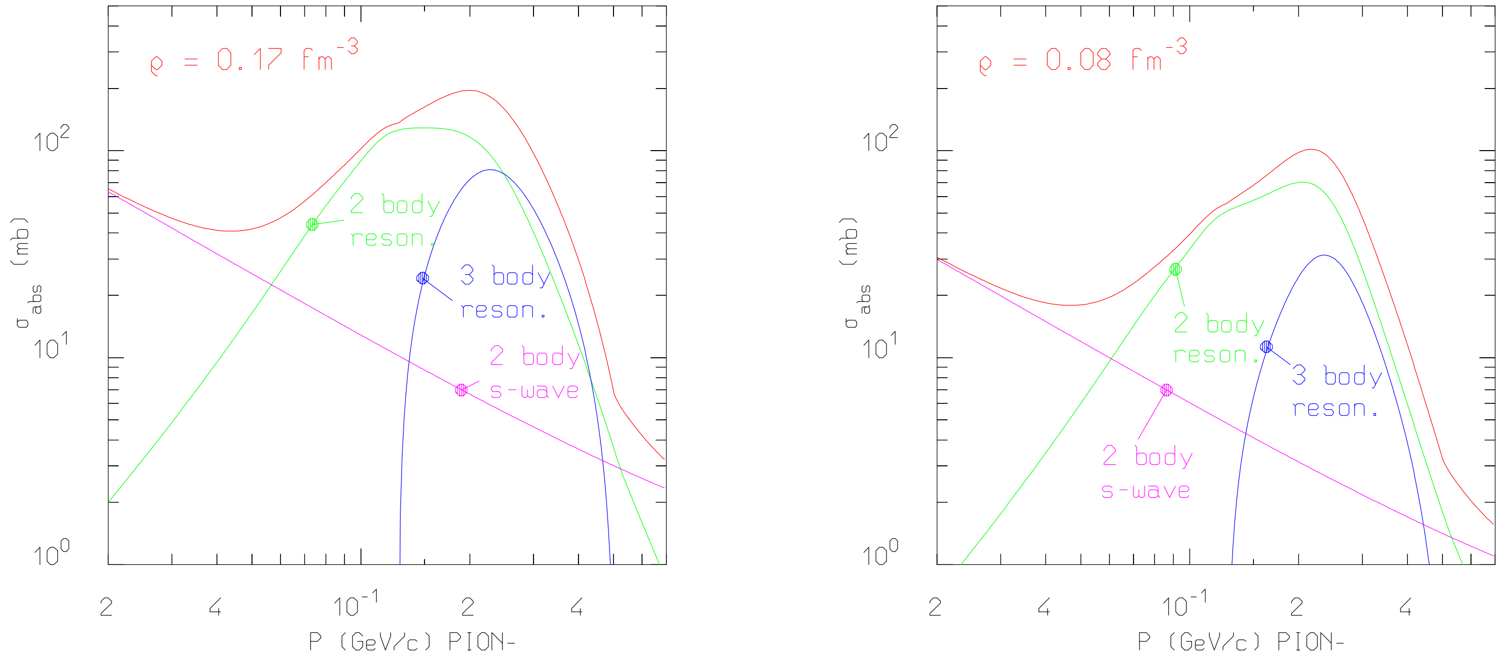

Charged pion absorption cross section for infinite symmetric nuclear matter at two different density values ($\lambda_{abs}^{-1} = \sigma_{abs} \cdot \frac{1}{2}\rho = \sigma_{abs} \cdot \rho_{pro} = \sigma_{abs} \cdot \rho_{neu}$)

Pion optical potential examples

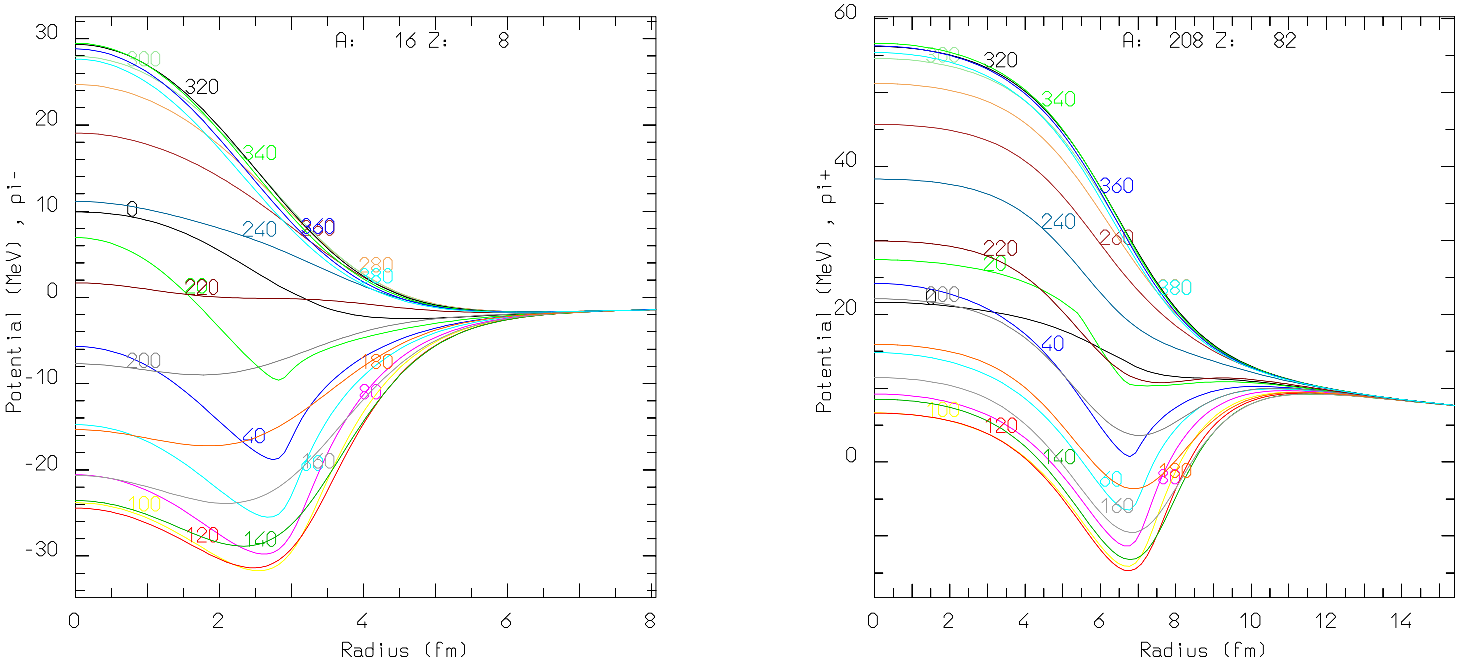

The real part of the pion optical potential for π^- on ^{16}O (left) and π^+ on ^{208}Pb (right) as a function of radius for various pion energies (MeV)

Pion absorption cross sections: examples

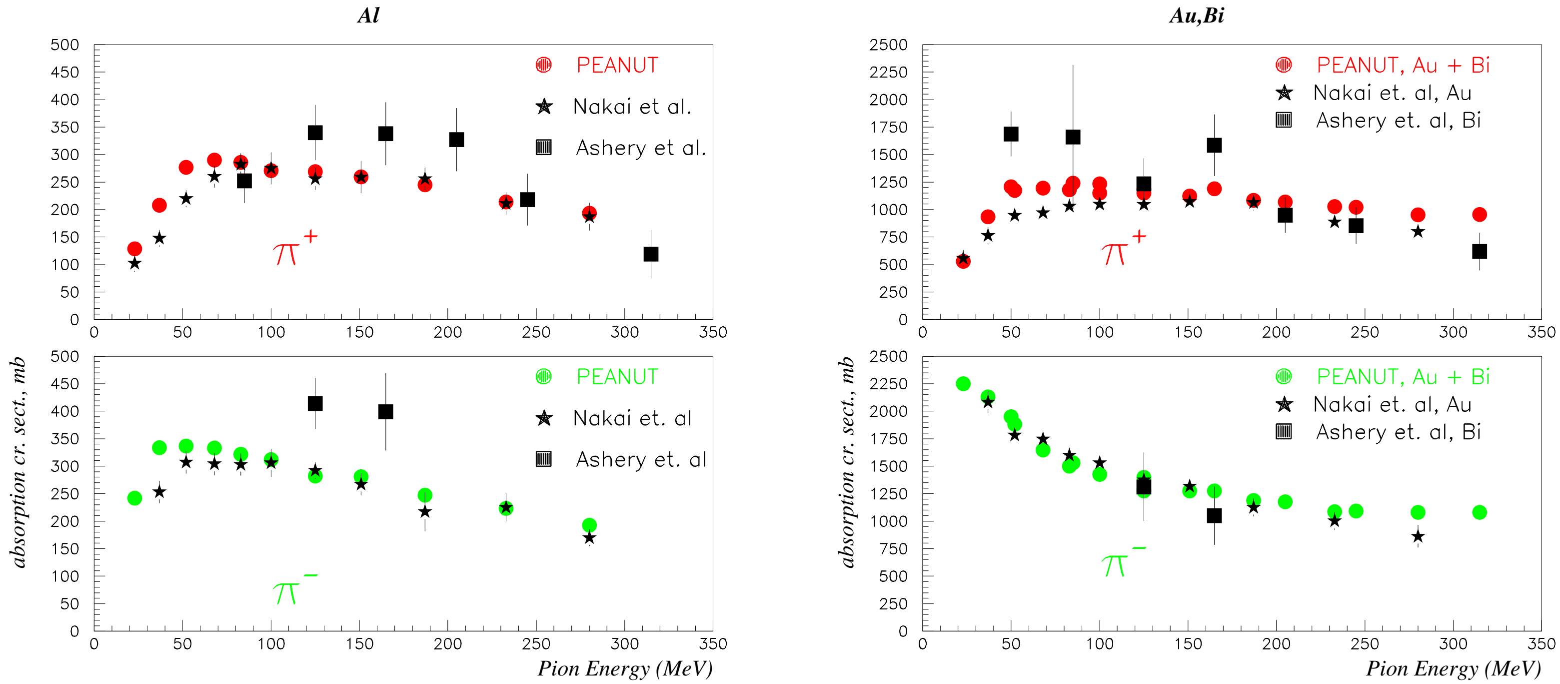

Computed and experimental pion absorption cross section on Aluminum as a function of energy

Computed and experimental pion absorption cross section on Gold or Bismuth as a function of energy

(Exp. data: D. Ashery et al., **PRC23**, (1981) 2173 and K. Nakai et. al., **PRL44**, (1979) 1446)

Pion-nucleus interactions: examples

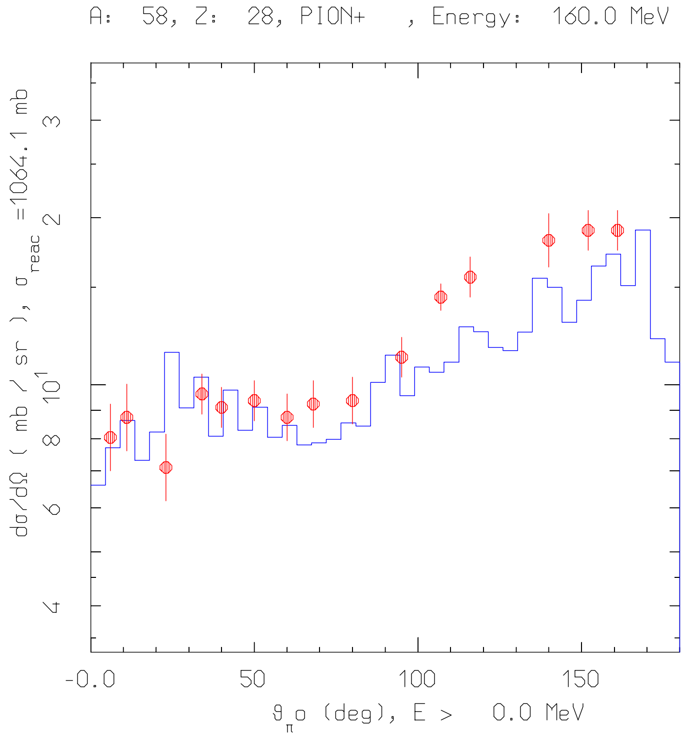

Computed and experimental pion charge exchange angular distribution for ^{58}Ni(π^+, π^0) at 160 MeV

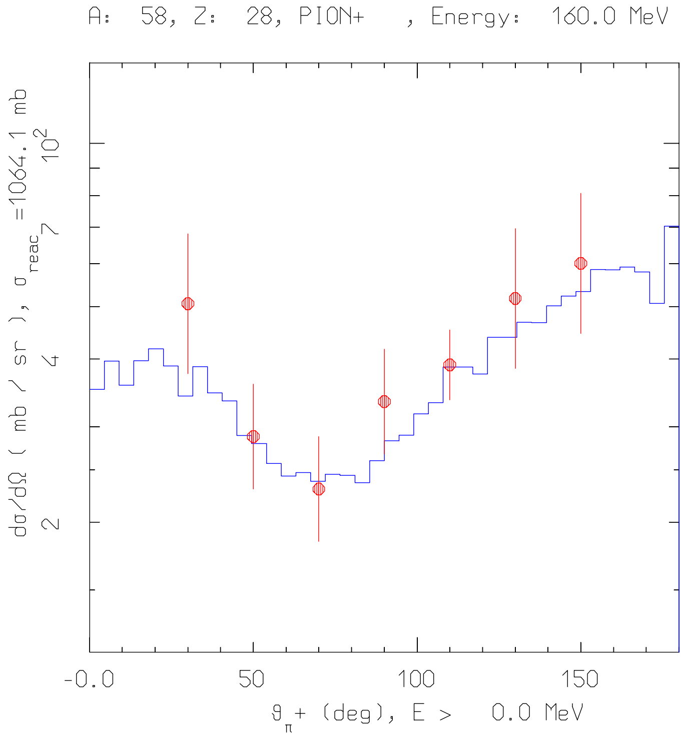

Computed and experimental pion inelastic angular distribution for ^{58}Ni$(\pi^+, \pi^{+\prime})$ at 160 MeV

Experimental data: Burger et al., **PRC41**, (1990) 2215 and McKeown et al., **PRC24**, (1981) 211

Positive Kaons: A probe of Fermi distribution

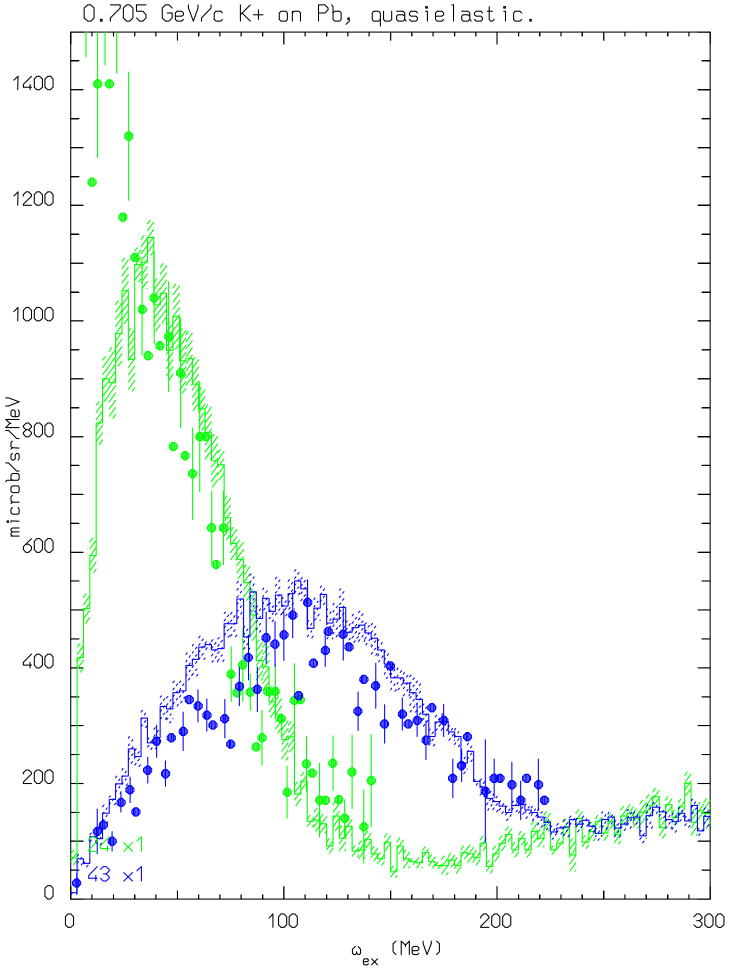

$K^+ \quad K^0$

No low mass S=1 baryons

$\rightarrow$ weak K^+N interaction

only elastic and charge exchange up to ≈ 800 MeV/c

$(K^+, K^{+\prime})$ on Pb vs residual excitation, 705 MeV/c, at $24°$ and $43°$.

Histo: FLUKA

Dots: data (Phys. Rev. C51, 669 (1995))

Corresponding recoil energy on free nucleon:
43 MeV at $24°$, 117 MeV at $43°$.

Preequilibrium

For E $>$ π production threshold $\rightarrow$ only (G)INC models

At lower energies $\rightarrow$ a variety of preequilibrium models

Two leading approaches

the quantum-mechanical multistep model	the exciton model
Very good theoretical background	statistical assumptions
complex, difficulties for multiple emission	simple and fast

- Exciton model: chain of steps, each (n_{th}) step corresponding to N_n "excitons" (exciton $=$ a particle above or a hole below the Fermi surface)
- Statistical assumption: any partition of the excitation energy among $N = N_h + N_p$ excitons has the same probability to occur
- Step: nucleon-nucleon collision with $N_{n+1} = N_n + 2$ (*"never come back"* approximation)
- Chain ends at equilibrium $=$ N_n sufficiently high or excitation energy below threshold

N_1 (initial configuration) depends on the reaction type and on the cascade history

Preequilibrium/(G)INC transition

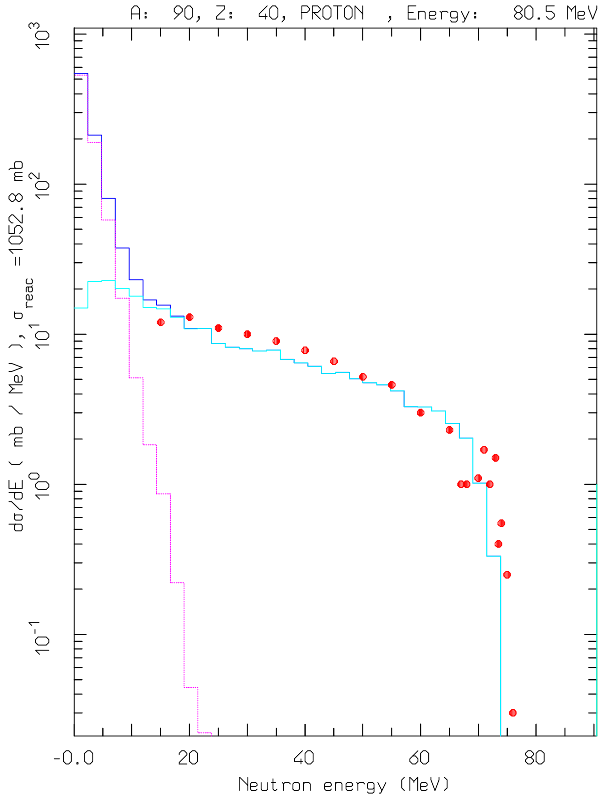

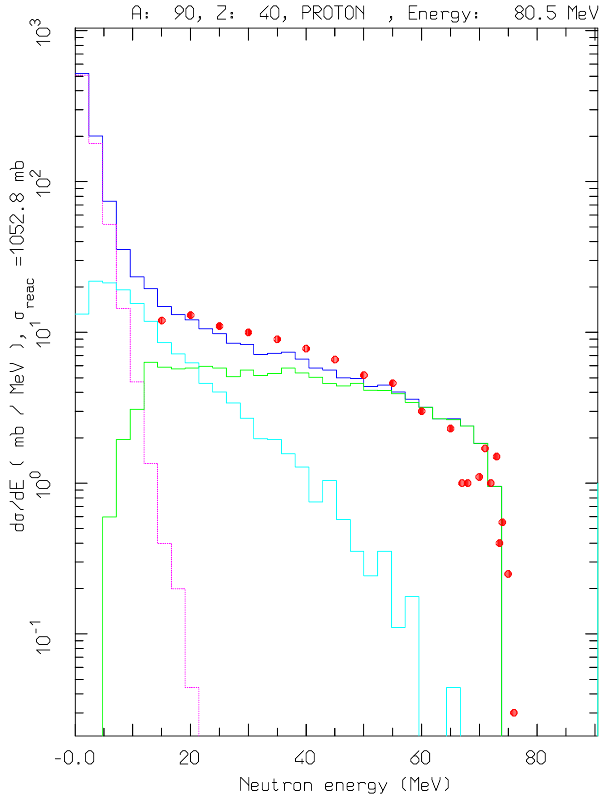

Angle integrated ^{90}Zr(p,xn) at 80.5 MeV calculations without the INC stage (left), and with the full algorithm (right). The various lines show the total, INC, preeq. and evaporation contributions
Experimental data from M.Trabandt et al. **PRC39** (1989) 452

Nonelastic interactions at intermediate energies: examples

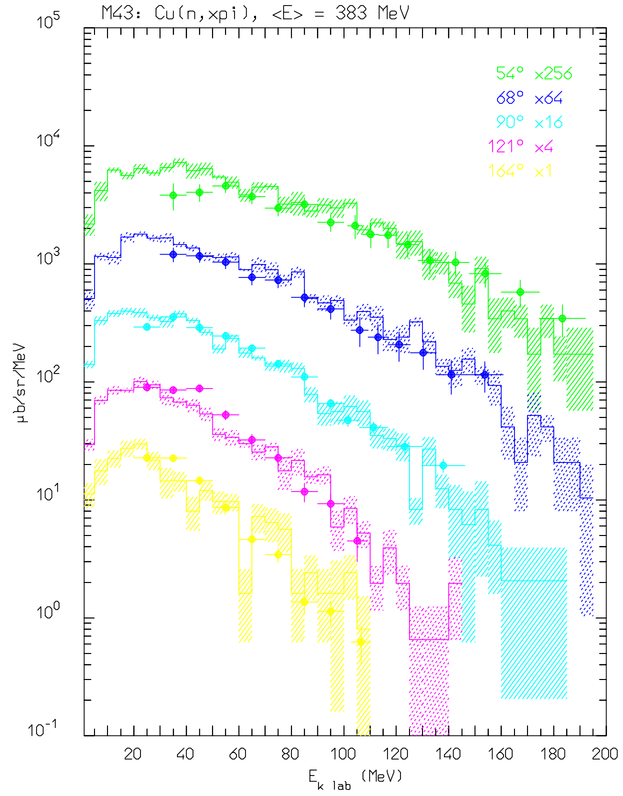

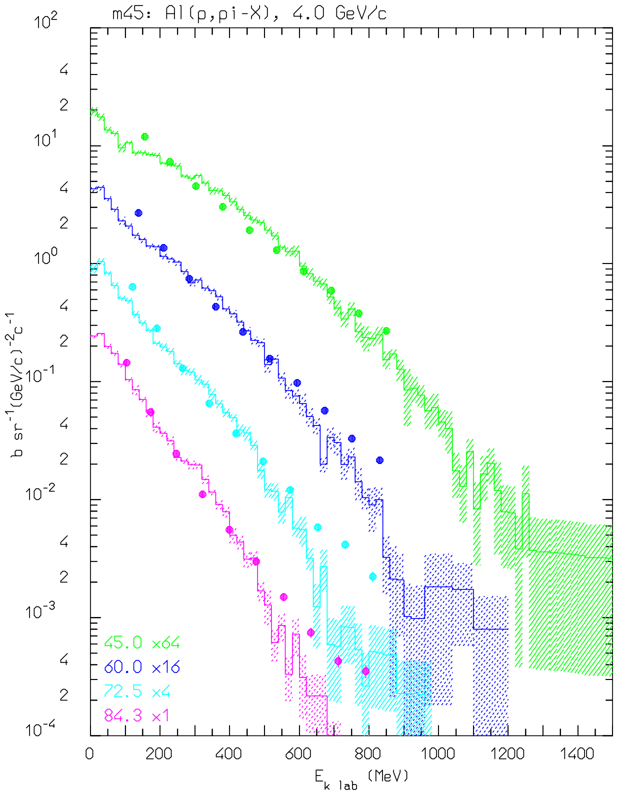

Double differential distributions of charged pions

Left: 383 MeV neutrons on Cu; Right: 4 GeV/c protons on Al

Experimental data from Buchle et al. **NPA515**, (1990) 541, and En'yo et al., PL 159B, 1 (1985))

Nucleon emission: thin target examples I

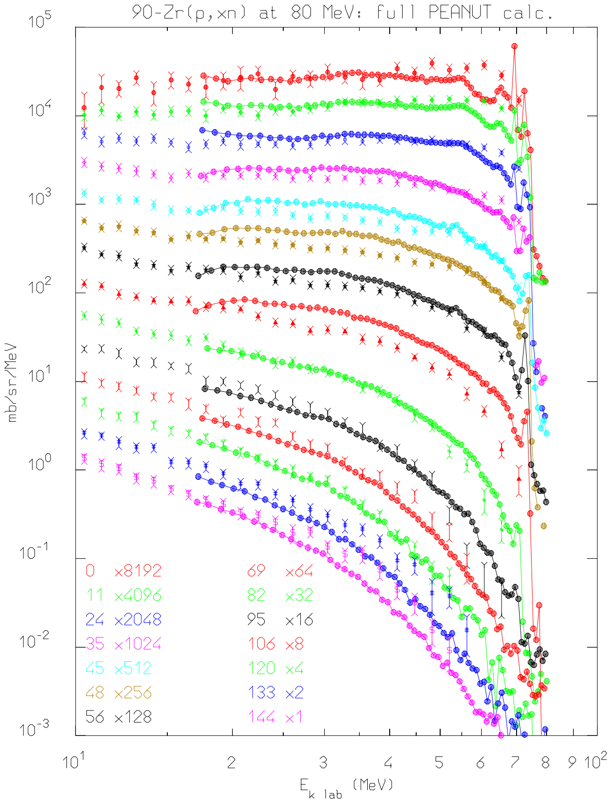

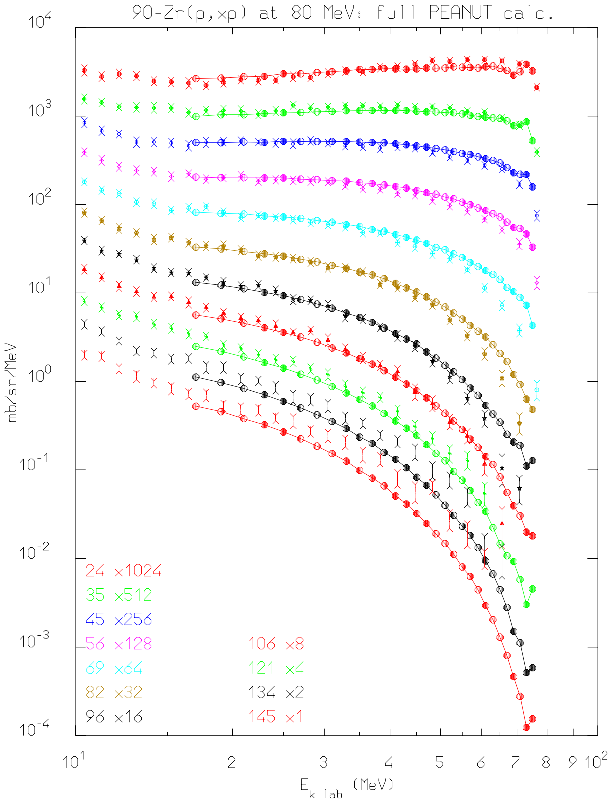

Double differential distributions at 80.5 MeV for ^{90}Zr(p,xn) (left) and ^{90}Zr(p,xp) (right)

Simple symbols: computed with FLUKA; symbols with lines: experimental data from M.Trabandt et al. **PRC39** (1989) 452 and A.A. Cowley et al., **PRC43**, (1991) 678

Nucleon emission: thin target examples II

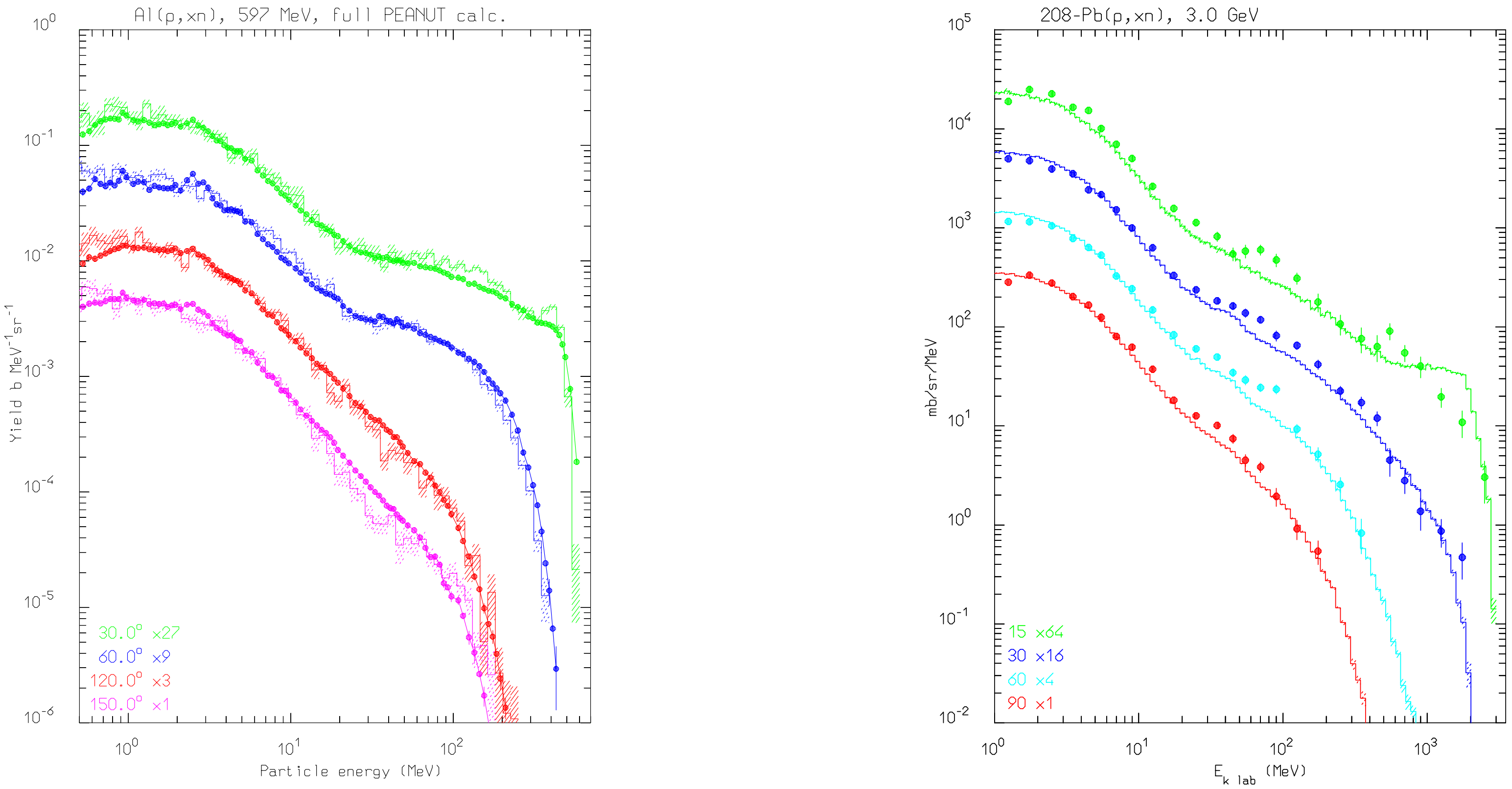

Double differential neutron distributions for Al(p,xn) at 597 MeV (left) and Pb(p,xn) at 3 GeV (right)

Histograms: computed with FLUKA; symbols: experimental data from

Amian et al., Nucl. Sci. Eng. **115**, (1993) 1, and Ishibashi et al., Nucl. Sci. Technol. **32** (1995) 827

Evaporation, fission and nuclear break-up

For a particle of type j , mass m_j, spin $S_j \cdot \hbar$ and kinetic energy E

(i for initial nucleus, f for final, F at fission saddle point):

Evaporation probability

$$P_j = \frac{(2S_j+1)m_j}{\pi^2\hbar^3} \int_{V_j}^{U_i-Q_j-\Delta_f} \sigma_{\mathsf{inv}} \frac{\rho_f(U_f)}{\rho_i(U_i)} E dE$$

Fission probability

$$P_F = \frac{1}{2\pi\hbar} \frac{1}{\rho_i(U_i)} \int_0^{(U_i-B_F)} \rho_F(U_i - B_F - E) dE$$

- ρ's: nuclear level densities,
- U: excitation energy,
- Δ: pairing gap,
- Q_j: reaction Q for emitting a particle of type j,
- σ_{inv}: cross section for the inverse process
- B_F: fission barrier
- V_j: (possible) Coulomb barrier for emitting a particle of type j

For low mass residuals: Fermi break-up: statistical phase-space production of multiple (excited) fragments

Excitation energy *after* evaporation $\rightarrow$ γ emission

Latest improvements to evaporation

- Improved state density $\rho = \exp(2\sqrt{aU})/U^{\frac{5}{4}}$
- No Maxwellian approximation for energy sampling
- γ competition
- Sub-barrier emission:

$$\sigma^x_{inv} = (R + \bar{\lambda})^2 \frac{\hbar\omega_x}{2E} \ln\left[1 + e^{\frac{2\pi(E - V_C)}{\hbar\omega_x}}\right]$$

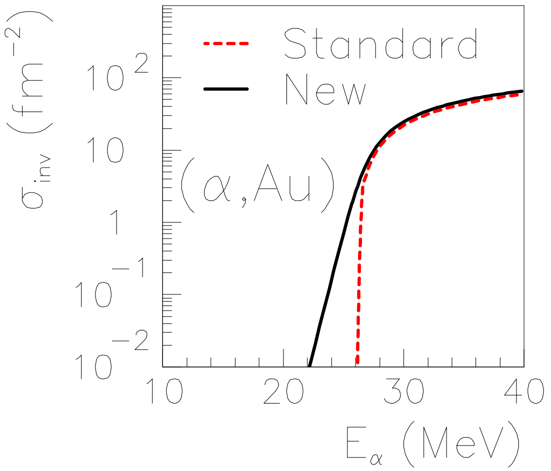

Neutron production examples: thick targets

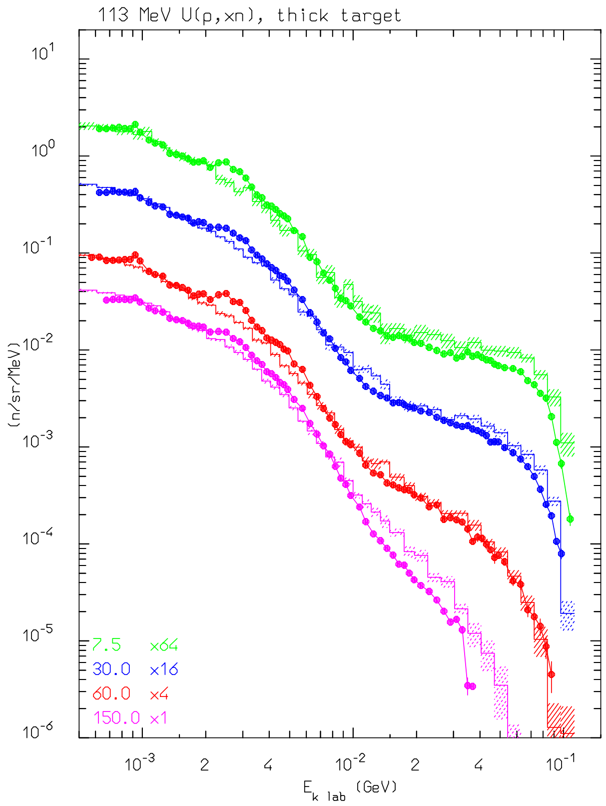

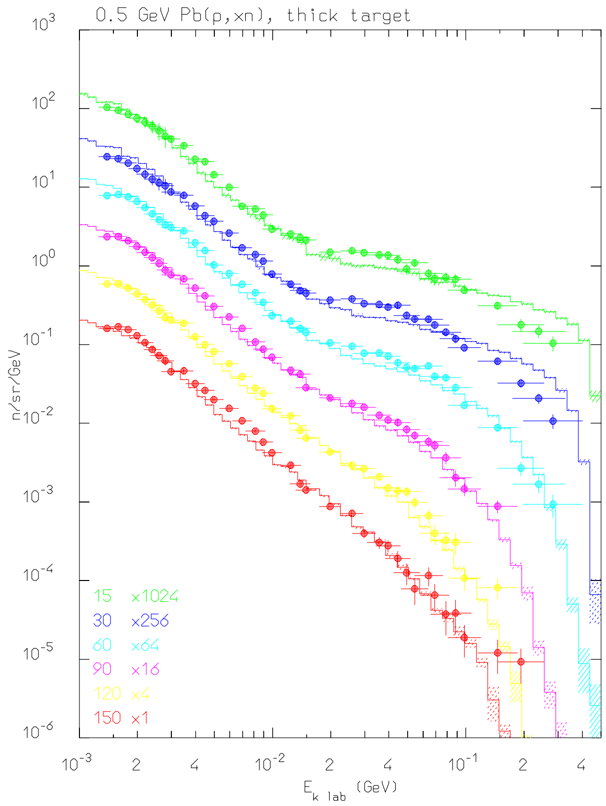

Neutron double differential distributions out of stopping length targets

Histogram: FLUKA simulation; symbols: experimental data

Left: 113 MeV protons on U (data from M.M. Meier et al., Nucl. Sci. Eng. **110**, (1992) 299)

Right: 500 MeV protons on Pb (S. Meigo et al., JAERI-Conf 95-008, (1995), 213)

High energy A-A interactions ($E > 5 - 10\ GeV/u$):

- Interface to DPMJET

Present

Intermediate energy A-A interactions

- Medium-heavy nuclei: interface to RQMD-2.4 code (H. Sorge)

- Medium-heavy nuclei: Internally developed QMD
- Light nuclei ($\leq$C): extension of PEANUT, (the FLUKA cascade+preequilibrium model)

Near Future

Low energy A-A interactions ($E < 100 MeV/amu$):

- Interface to Monte-Carlo Boltzmann Master Equation code developed at Milan University (NPA 679 (2001) 753)

DPMJET: *(R. Engel, J. Ranft, and S. Roesler)* [1]:

Nucleus-Nucleus interaction code for collisions from ≈5-10 GeV/n up to the highest cosmic ray energies ($10^{18} - 10^{20}$ eV). Used in many CR shower codes

Based on the Dual Parton Model and the Glauber model, like the high energy FLUKA hadron-nucleus generator. Two-component DPM approach (soft and pQCD)

FLUKA-DPMJET

(DPMJET-II.53, upgrading to DPMJET-III):

Cross sections pre-computed by DPMJET→ tabulation for FLUKA of a full projectile/target matrix up to A = 246

Glauber impact parameter distributions pre-computed over complete A and E range

Interface call at beginning and end of single interactions

Reaction products given back to be transported by FLUKA

Evaporation and deexcitation of residual nuclei performed in FLUKA

[1] PRD 51 (1995) 64; Gran Sasso INFN/AE-97/45 (1997); hep-ph/9911232; hep-ph/9911213; hep-ph/0002137, "The Monte Carlo Event Generator DPMJET-III" Proc. MC2000, Springer-Verlag Berlin, Heidelberg, pp. 1033-1038

DPMJET-III: examples of performances

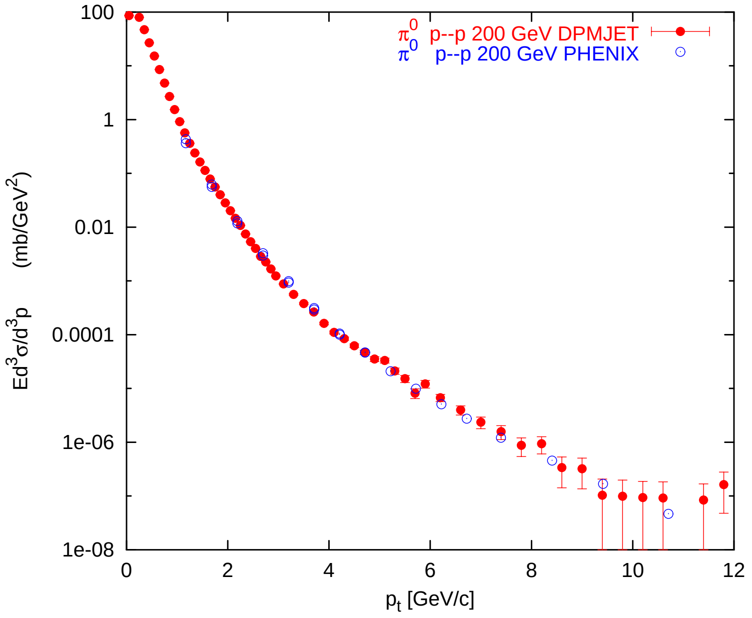

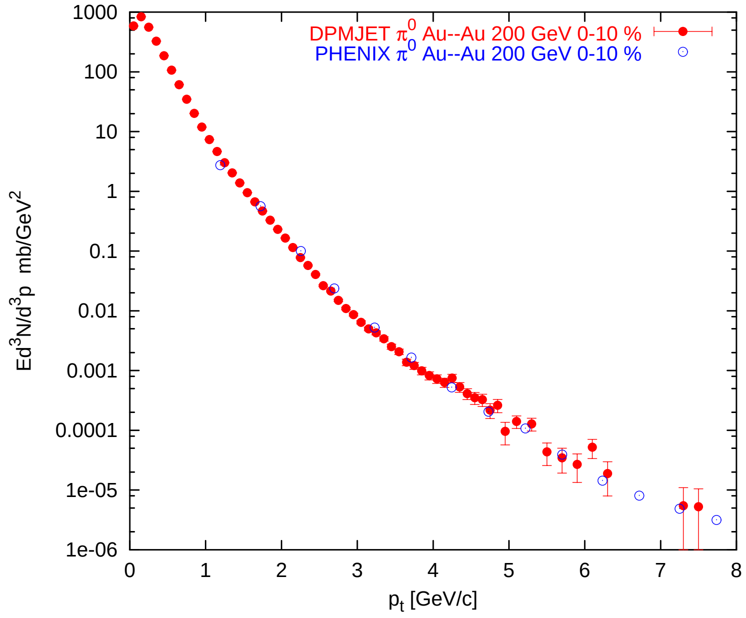

Invariant cross section for π^0 production as a function of p_t for hadron-hadron and nucleus-nucleus collisions

Left: 200 GeV p-p; Right: 200 Gev Au-Au (of 0–10% centrality)

Red: DPMJET calculations; Blue: experimental data from PHENIX

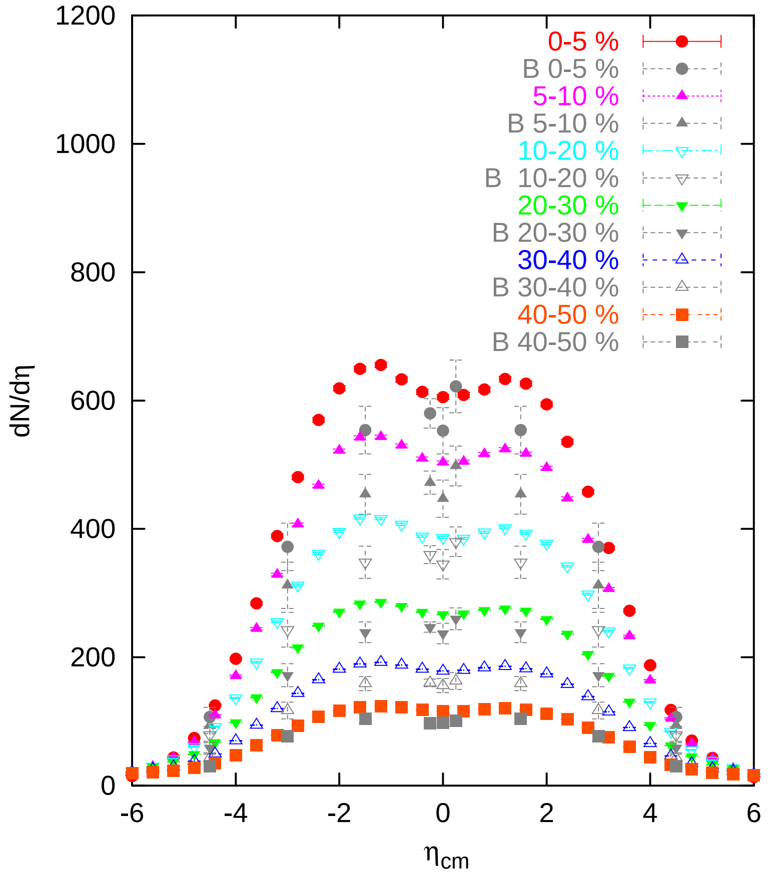

Pseudorapidity distributions of charged hadrons in Au–Au collisions at $\sqrt{(s)}= 130$ GeV for centralities 0–5 % up to 40–50 %.

Colored points are from the DPMJET-III Monte Carlo with chain fusion.

Data points (with a B in the label) from the BRAHMS, PHENIX and PHOBOS Collaborations

(r)QMD approach:

Features of a generic QMD:

- Nucleons = wave packets
- Classical Hamilton equations of motion
- Mean field potential given by sum of:
  two-body + three-body + surface + Coulomb + Fermi

$\Rightarrow$ the mean field evolves during the interaction

Introduce (Monte Carlo) two–body scattering/interactions to model the reaction

Initialization is critical (very unstable configurations possible)
Relativistic extension problematic.

... RQMD-2.4 (next slide) is a (relativistic) QMD model with some of these features

The FLUKA–RQMD-2.4 interface

Author: H. Sorge (PRC52 3291 (1995), Ann. Phys. 192 266 (1989))

Relativistic QMD model applicable from ≈ 0.1 GeV/n up to several hundreds of GeV/n, successfully applied to relativistic A-A particle production over a wide energy range

Problems:

- No evaporation/fragmentation/fission/deexcitation of residuals and fragments
- Serious energy non-conservation issues, particularly when run in full QMD mode
- No meaningful excitation energy calculation implemented or possible
- No longer maintained

Solutions:

- Rework from scratch the nuclear final state out of the available info on spectators, correlating the excitation energy to the actual hole depth of hit nucleons
- Fix the remaining energy-momentum conservation issues taking into account exp. binding energies as well
- Use the FLUKA evaporation/fragmentation/fission/deexcitation module

Temporary solution for A-A interactions below few GeV/n

FLUKA with modified RQMD-2.4 - results

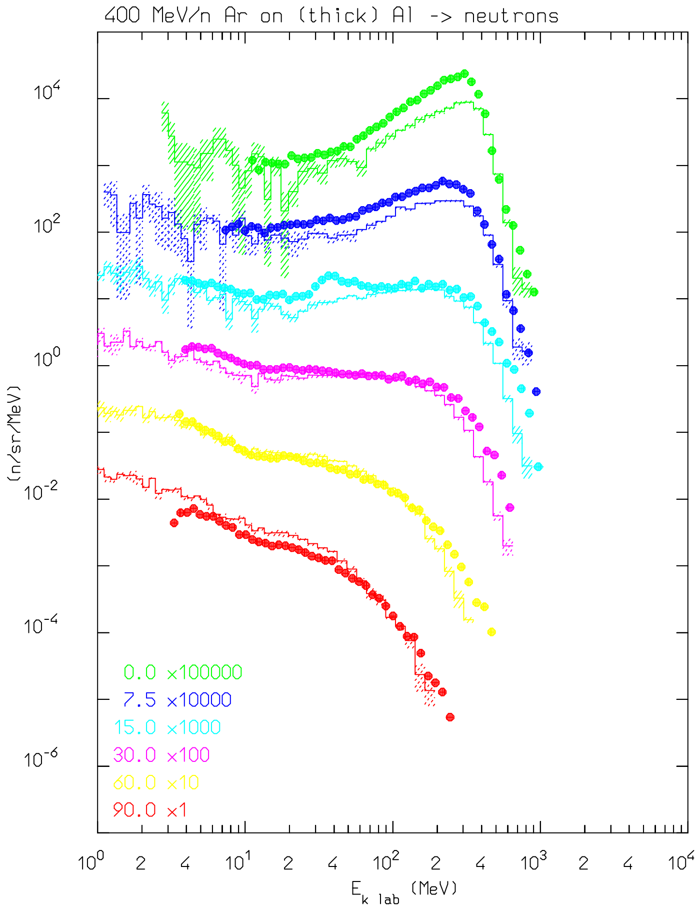

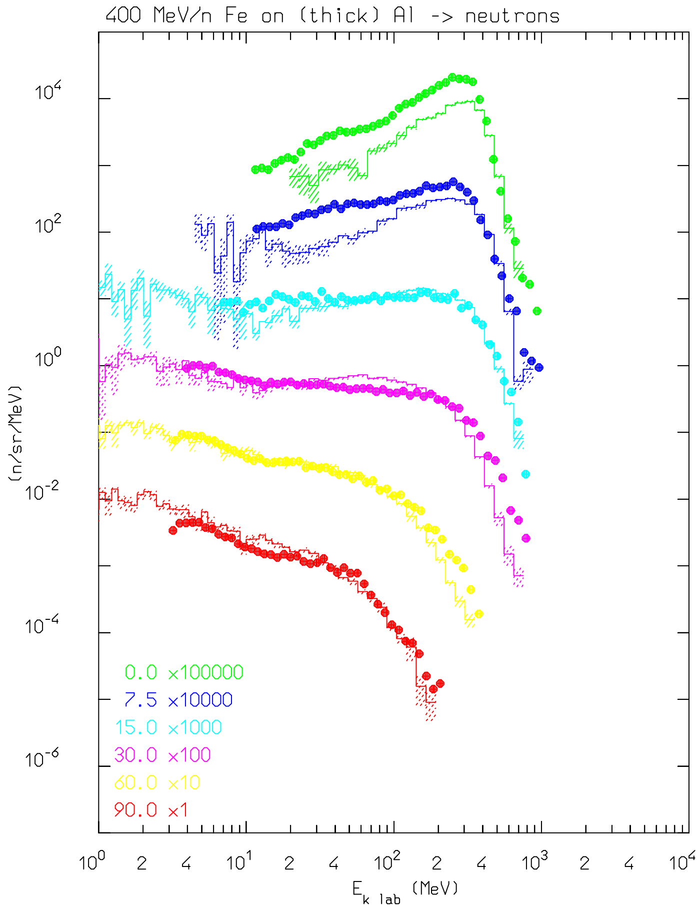

Double differential neutron yield by 400 MeV/n Ar (left) and Fe (right) ions on thick Al targets
Histograms: FLUKA; Dots: experimental data (PRC62 044615 (2000))

FLUKA with modified RQMD-2.4 - results II

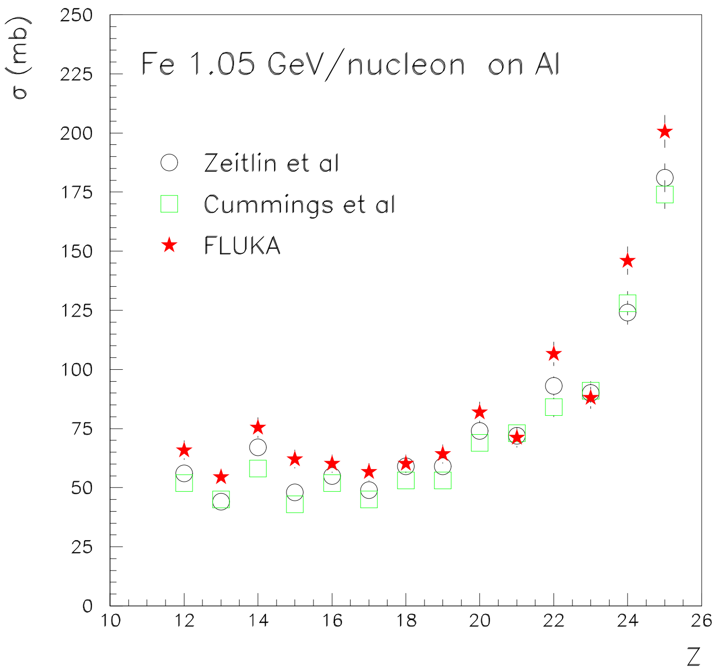

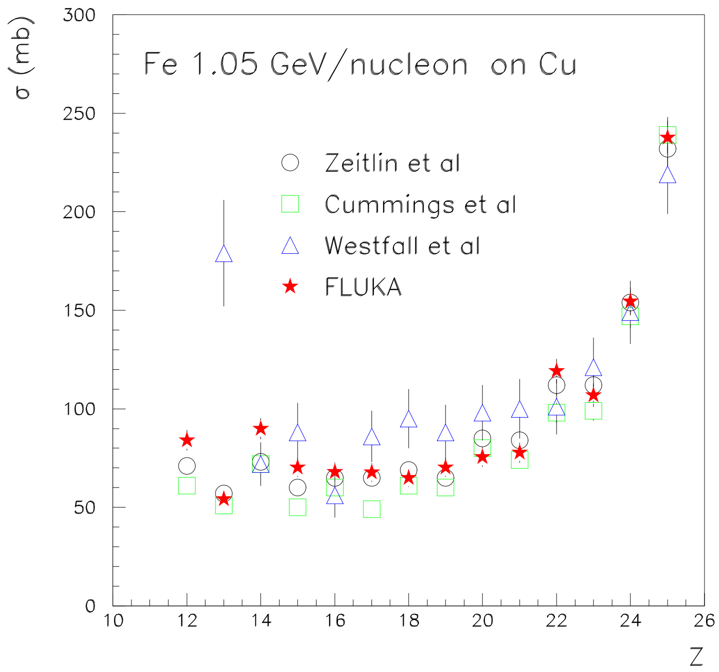

Fragment charge cross sections for 1.05 GeV/n Fe ions on Al (left) and Cu (right) stars FLUKA, circles PRC56 (1997) 388, squares PRC42 (1990) 5208 (at 1.5 GeV/n), triangles PRC19 (1979) 1309 (at 1.88 GeV/n).

Monte Carlo BME

Monte Carlo based on the **B**oltzmann **M**aster **E**quation theory

Heavy ion reactions at incident energies of a few tens of MeV/amu

BME: statistical evolution of the composite nucleus through a sequence of two body interactions and emission of unbound particles, also in the form of light clusters. Mean field effects are taken into account

BME is inclusive, but:

Milan: Monte Carlo calculation applies the BME theory on very small time intervals $\rightarrow$ *exclusive, correlated events*

Includes incomplete fusion processes following the projectile break-up

M. Cavinato et al., Nucl. Phys. A 679 (2001) 753

M. Cavinato et al., Phys. Lett. B 382 (1996) 1

E. Gadioli et al., Nucl. Phys. A, in press

Monte Carlo BME: examples from Nucl. Phys. A 679 (2001) 753

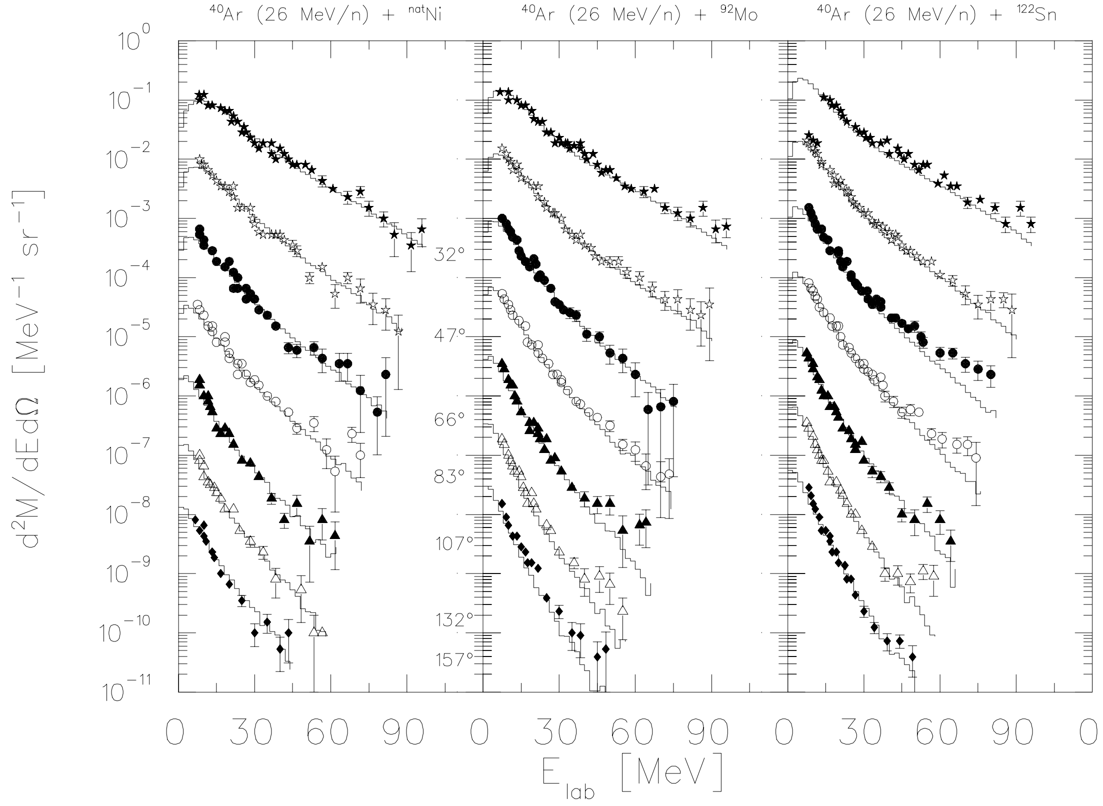

Spectra of neutrons emitted in central collisions of ^{40} Ar with Ni, ^{92}Mo and ^{122}Sn at 26 MeV/amu

Symbols: experimental data, histograms: simulation results.

Starting from top the spectra are progressively scaled down by a factor 10

Muon Capture

An exotic source of neutron background *(e.g., background at nTOF)*

Basic weak process : $\mu^- + p \rightarrow \nu_\mu + n$

μ^- at rest $+$ atom $\rightarrow$ excited muonic atom $\rightarrow$ x-rays+g.s muonic atom

Competition between μ decay and μ capture by the nucleus.

In FLUKA: Goulard-Primakoff formula

$\Lambda_c \propto Z^4_{eff}$, calculated Z_{eff}, Pauli blocking from fit to data.

$\frac{\Lambda_c}{\Lambda_d} = 9.2 \cdot 10^{-4}$ for H, 3.1 for Ar, 25.7 for Pb

Nuclear environment (Fermi motion, reinteractions, deexcitation. . .)

from the FLUKA intermediate-energy module PEANUT

Slow projectile, low energy transfer (neutron E=5 MeV on free p)

Experimentally: high energy tails in n-spectra

Beyond the simple one-body absorption

Good results from addition of two-nucleon absorption

Muon Capture: comparison with data

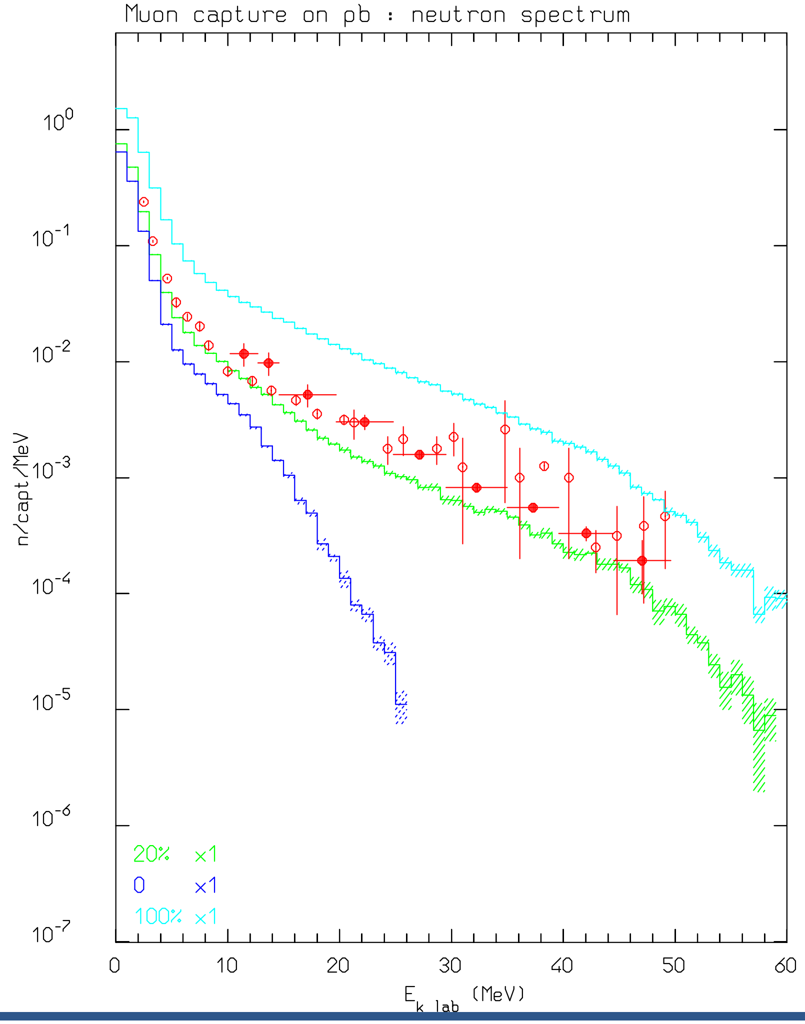

Neutron spectra following muon capture on Lead

Dots: experimental data

Histograms: FLUKA calc.

The three curves correspond to a percentage of 2-body absorption of 0, 20%, and 100% .

Emitted:

1.7 neutrons/capture

0.002 protons/capture

nTOF ^{3}He: measured vs simulated time spectra

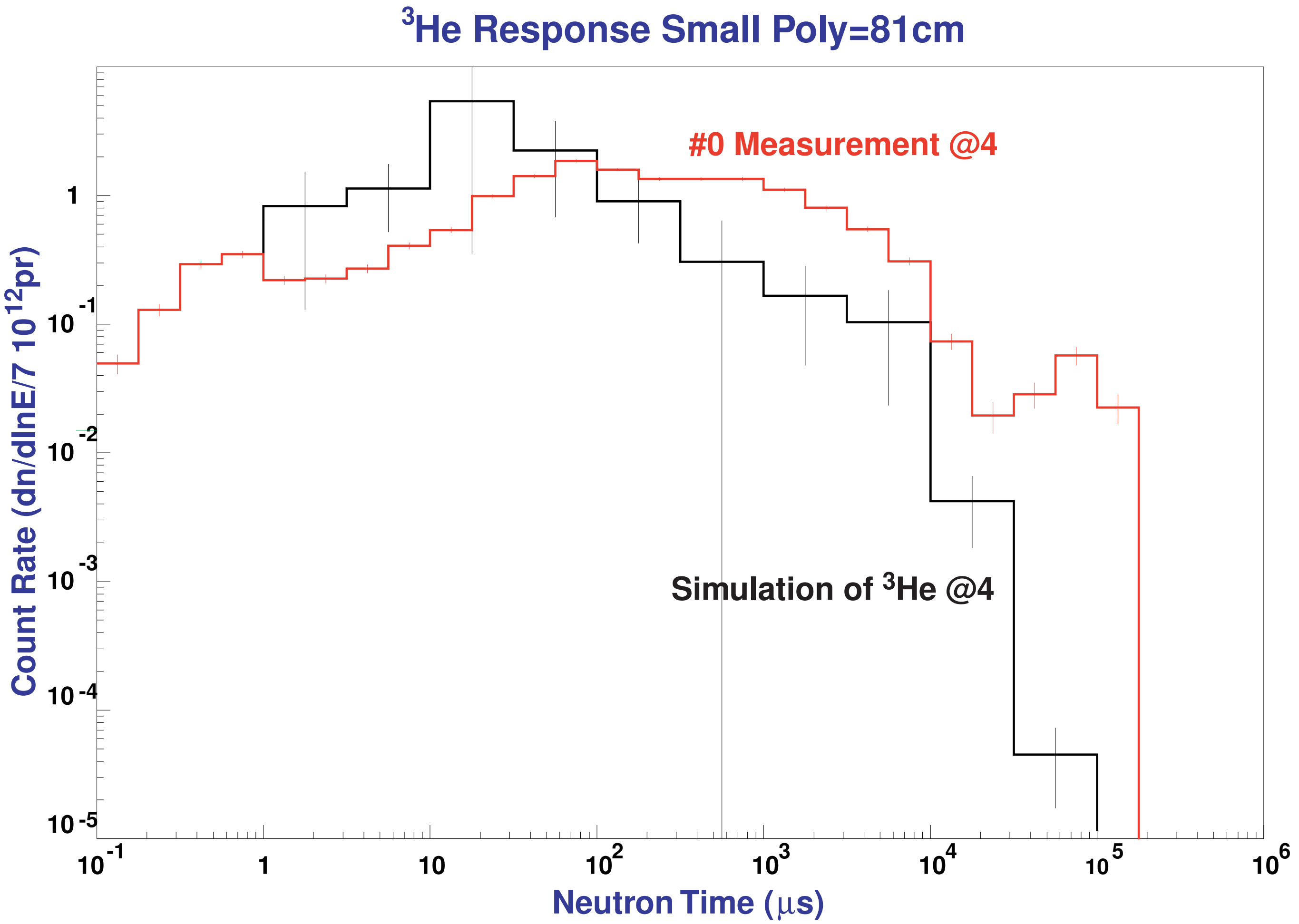

Measured (red) versus computed (black) ^{3}He + poly. 81 mm time spectra
The comparison is absolute